Rock Mechanics and Rock Engineering

Poroelastic Properties of Sierra White Granite

--Manuscript Draft--

Manuscript Number:	RMRE-D-23-00687
Full Title:	Poroelastic Properties of Sierra White Granite
Article Type:	Original Paper
Keywords:	Skempton's B, Biot's effective stress coefficient, Poroelasticity, Grain bulk modulus, Sierra White granite
Manuscript Classifications:	100.020: Laboratory testing; 500.010: Petroleum rock mechanics; 500.020: Geothermal systems; 500.060: Hydraulic fracturing; 500.070: Induced seismicity
Corresponding Author:	Ahmad Ghassemi University of Oklahoma Norman, OK UNITED STATES
Corresponding Author Secondary Information:	
Corresponding Author's Institution:	University of Oklahoma
Corresponding Author's Secondary Institution:	
First Author:	Ahmad Ghassemi
First Author Secondary Information:	
Order of Authors:	Ahmad Ghassemi
	Xuejun Zhou, Ph.D.
Order of Authors Secondary Information:	
Funding Information:	
Abstract:	In this work, poroelastic properties of Sierra White granite are determined, including elastic moduli, Biot's effective stress coefficient, α, and Skempton's pore pressure coefficient, B. The Biot's coefficient of this rock was determined using two different approaches. It is found that overall, the Biot's coefficient decreases from 0.77 at low effective stress (3~4 MPa) to 0.45~0.55 at high effective stress levels (30~40 MPa). Unlike the Biot's effective stress coefficient, which is related only to the solid rock, Skempton's B is a property related to both solid rock and pore fluid. Although a single undrained hydrostatic compression test can theoretically be used to measure B, two types of laboratory tests were performed to fully reveal this parameter's behavior. In the first test, the back pressure and confining pressure are increased stepwise to maintain a constant effective stress (usually very low), and Skempton's B is measured at different back pressure levels. This test reveals the Skempton's B behavior related to pore fluid compressibility, and consequently, this test can be used to evaluate if the pore fluid is free of air. In the second test, the back pressure is maintained at a constant level, and the confining pressure is increased stepwise, and then Skempton's B is determined at different confining pressure levels. This test correlates Skempton's B with effective stresses. Details of the laboratory test protocol for combining these two types of tests are described and the results for Sierra White granite are provided. It is found that for Sierra White granite, the Skempton's B falls in a narrow range of 0.8~0.86 in the first test after the pore fluid is depleted of air; while in the second test it falls in a large range (0.86 to a lower value depending on the effective stresses).

This paper has been submitted to RMRE for Review on 05/22/2023

Poroelastic Properties of Sierra White Granite

Xuejun Zhou · Ahmad Ghassemi*

Reservoir Geomechanics and Seismicity Group,
The University of Oklahoma, Norman, OK, USA

Abstract

In this work, poroelastic properties of Sierra White granite are determined, including elastic moduli, Biot's effective stress coefficient, α, and Skempton's pore pressure coefficient, B. The Biot's coefficient of this rock was determined using two different approaches. It is found that overall, the Biot's coefficient decreases from 0.77 at low effective stress (3~4 MPa) to 0.45~0.55 at high effective stress levels (30~40 MPa). Unlike the Biot's effective stress coefficient, which is related only to the solid rock, Skempton's B is a property related to both solid rock and pore fluid. Although a single undrained hydrostatic compression test can theoretically be used to measure B, two types of laboratory tests were performed to fully reveal this parameter's behavior. In the first test, the back pressure and confining pressure are increased stepwise to maintain a constant effective stress (usually very low), and Skempton's B is measured at different back pressure levels. This test reveals the Skempton's B behavior related to pore fluid compressibility, and consequently, this test can be used to evaluate if the pore fluid is free of air. In the second test, the back pressure is maintained at a constant level, and the confining pressure is increased stepwise, and then Skempton's B is determined at different confining pressure levels. This test correlates Skempton's B with effective stresses. Details of the laboratory test protocol for combining these two types of tests are described and the results for Sierra White granite are provided. It is found that for Sierra White granite, the Skempton's B falls in a narrow range of 0.8~0.86 in the first test after the pore fluid is depleted of air; while in the second test it falls in a large range (0.86 to a lower value depending on the effective stresses).

Highlights

- The development of laboratory test protocol for Skempton's B measurement with a consideration of both fluid and solid properties.
- A comparison of using two different approaches to measure the Biot's effective stress coefficient.
- Determination of Biot's effective stress coefficient, α, and Skempton's pore pressure coefficient, B, for Sierra White granite.

Keywords Skempton's B, Biot's effective stress coefficient, Poroelasticity, Grain bulk modulus, Sierra White granite

*Corresponding author email: ahmad.ghassemi@ou.edu (Ahmad Ghassemi) Phone: 405-325-4347

List of symbols

B	Skempton's B
H	Poroelastic expansion coefficient
K	Drained bulk modulus
K_f	Pore fluid bulk modulus
$K_s^{'}$	Grain bulk modulus
$1/K_s^{''}$	Unjacketed pore compressibility
m_f	Mass of pore fluid
P_c	Confining pressure
P_p	Pore pressure
V_ϕ	Pore volume
α	Biot's effective stress coefficient
σ^{eff}	Effective stress
σ	Stress
ϕ	Porosity
ε_v	Volumetric strain

1. Introduction

Two key parameters that are of interest for the poroelastic analysis in rock are Skempton's B and Biot's effective stress coefficient, α (Biot 1941; 1957; Skempton 1954; Ghassemi et al. 2009). If a fluid-saturated porous rock undergoes undrained hydrostatic compression, the confining pressure causes the pores to contract, thereby pressurizing the trapped pore fluid. The magnitude of this induced pore-pressure increment is described by the following equation (Berge et al. 1993; Skempton 1954; Cheng 2016):

$$B = \left.\frac{\Delta P_p}{\Delta P_c}\right|_{\Delta m_f = 0} \tag{1}$$

where m_f is the mass of pore fluid (zero implies undrained condition), P_c and P_p are the confining pressure and pore pressure, respectively. It should be noted that Skempton's B is related with both rock matrix and pore fluid properties. The relationships among Skempton's B and compressibility or drained bulk moduli of bulk rock, solid grain, and pore fluid, as well as porosity, have been investigated by many researchers (Brown and Korringa 1975; Rice and Cleary 1976; Berryman and Milton 1991; Berge et al. 1993). And the relationship among these quantities can be described as:

$$B = \frac{\frac{1}{K} - \frac{1}{K_s^{'}}}{\frac{1}{K} - \frac{1}{K_s^{'}} + \phi\left(\frac{1}{K_f} - \frac{1}{K_s^{''}}\right)} \tag{2}$$

where ϕ is the porosity, K is the drained bulk modulus of rock, $K_s^{'}$ is the solid grain bulk modulus or unjacketed solid frame bulk modulus, $1/K_s^{''}$ is the unjacketed pore compressibility, which is defined as $K_s^{''} = -V_\phi(\partial P_f / \partial V_\phi)_{dP_f = dP_c}$; and K_f is pore fluid bulk modulus. If all grains in the rock are composed of the same material, $K_s^{'} = K_s^{''}$(Berge et al. 1993). It is believed that any difference between $K_s^{'}$ and $K_s^{''}$is a result of deviation from an ideal porous material assumption, which refers to such a type of material with a uniform, isotropic and linearly elastic solid phase and a fully connected porous space (Cheng, 2016; Makhnenko et al. 2017; Tarokh et al. 2018). Note in this equation, both fluid property (K_f) and rock frame property (K , $K_s^{'}$, $K_s^{''}$) can all have impact to *B*. When the fluid compressibility is extremely small (such as gas with $K_f \to 0$), the denominator could become very large thus making *B* very small. That is, a variation of pore fluid could result in a fluctuation of Skempton's *B*.

The Skempton's *B* that is commonly referred to in the literature is usually based on the condition of water as the pore fluid. The Skempton's *B* coefficient allows the coupling between mechanical deformation and pore pressure to be quantified (Jaeger et al. 2007).

Biot's effective stress coefficient, α, is a key parameter that quantifies the contribution of the pore pressure to the effective stress. Biot's coefficient is a property of the solid and the porous frame only, which is independent of the fluid properties (Cheng 2016; Coussy 2004). Thus, the type of pore fluids (water, gas, or a mixture of different fluids) have no impact to the Biot's coefficient's measurement provided no physical/chemical reactions take place between the rock frame and the pore fluid(s). Assuming the effective-stress law is known, then the rock behavior can be measured at one pore pressure (often zero) and subsequently predicted for any other pore pressure. The Biot's effective stress law is usually given as (Biot 1941; 1957):

$$\sigma^{eff} = \sigma - \alpha P_p \qquad (3)$$

where σ is the stress, and σ^{eff} is the effective stress. Biot's effective stress coefficient has been measured for many different types of rocks using various methods based on different formulas (Blocher et al. 2014; Cheng et al. 1993; 1997; Zhou and Ghassemi 2015; 2022). A widely used formula for the estimation of the α is the following equation:

$$\alpha = 1 - \frac{K}{K_s^{'}} \qquad (4)$$

Since both K and $K_s^{'}$ are rock solid properties, α is independent of the pore fluid from a theoretical standpoint.

In another approach, α is expressed as a ratio of the drained bulk modulus K and the poroelastic expansion coefficient H (Wang 2000).

$$\alpha = \frac{K}{H} \qquad (5)$$

where H is called the poroelastic expansion coefficient, which describes how much the bulk volume changes due to a pore pressure change while holding the applied stress constant (note that Wang (2000) names H as the reciprocal of poroelastic expansion coefficient, and here we refer H as poroelastic

expansion coefficient for simplicity. We also treat H as an absolute positive number). Poroelastic expansion coefficient is the ratio of the pore pressure change over the volumetric strain under a constant confining pressure condition.

$$H = \frac{\Delta P_p}{\frac{\Delta V}{V}} = \left.\frac{\Delta P_p}{\Delta \varepsilon_V}\right|_{\Delta Pc=0} \qquad (6)$$

This parameter can be measured in the laboratory by conducting a pore fluid depletion test. Furthermore, a hydrostatic compression test for measuring K and a hydrostatic depletion test for measuring H can form a pair of tests for the measurement of α provided the confining and pore pressure levels are comparable for these two types of tests.

2. Sample information

Sierra White granite is mined and quarried from the granite rich Sierra Nevada mountain range in the USA, and is widely used as a construction material and rock mechanical studies. The samples information is summarized in the following Table 1 and Figure 1. This type of rock's permeability is extremely low, in the nano Darcy range (Hu and Ghassemi 2019; Ye and Ghassemi 2018). These samples appear to be homogeneous and isotropic. The mineralogy information is listed in the following Table 2.

Table 1. Sample information.

Sample No.	Length (mm)	Diameter (mm)	Weight (g)	Density (g/cm^3)
A	73.40	37.70	215.51	2.63
C	68.60	37.70	202.02	2.63

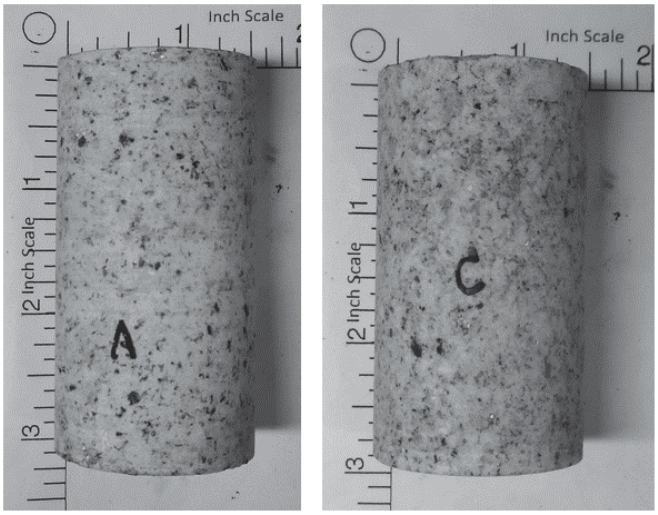

Fig.1 Sample image (These two samples are retrieved from a same block; Sample A was tested for Skempton's *B* and Sample C was tested for the Biot's effective stress coefficient. These two tests are independent with respect to each other. The Skempton's *B* measurement requires full water saturation on Sample A, while argon was used as the pore fluid for the Biot's coefficient measurement on Sample C)

Table 2. Mineralogy of the Sierra White granite (Ye and Ghassemi, 2018).

Sierra White granite	
Quartz	43.5%

Albite	46.1%
Sanidine	4.8%
Biotite	2.7%
Illite	2.0%
Clinochlore	0.9%

3. Laboratory test procedure

Laboratory test procedures of Skempton's *B* and the Biot's effective stress coefficient are different and are described in the following two sections.

3.1 Skempton's *B* measurement

Laboratory measurement of Skempton's *B* requires a full saturation of the rock samples. After a few trials, methods have been developed with some variations based on the conventional saturation method and some previous studies (ASTM 2004; Hart and Wang 1995; Mesri et al. 1976; Tarokh et al. 2018).

For a rock of low permeability, the test of Skempton's *B* is difficult and challenging. Unlike Biot's coefficient, which is a property of the solid rock only, Skempton's *B* is influenced by both rock matrix property and pore fluid property. Using different pore fluids (water, oil, or water with different gas/air concentration) will yield different *B* values. To make the results reliable and more meaningful with respect to the real-world applications, pure water saturation is desired, although this could be quite difficult for rock samples of low permeability and porosity. The workflow can be described by the following flowchart (Figure 2).

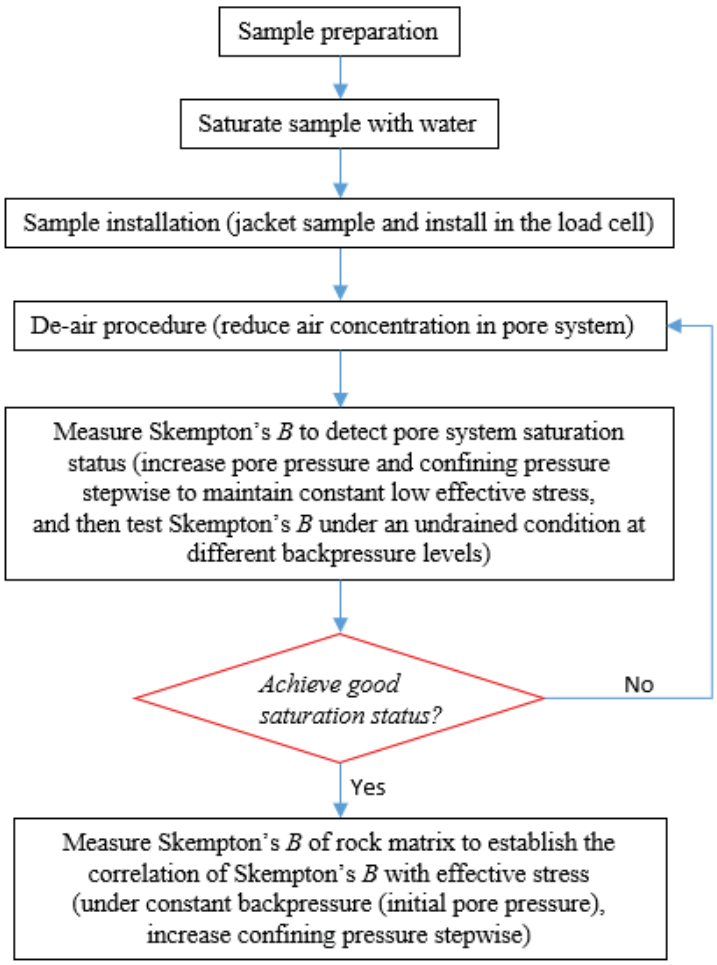

Fig.2 Laboratory test procedure flowchart (There are two sections of measuring the Skempton's *B*: the first one (Box 5) on the impact of pore fluid compressibility to the Skempton's *B*, and the second one (Box 7) on the impact of rock structure to the Skempton's *B*).

The sample is prepared in a cylinder shape with both end surfaces polished according to the rock mechanic test requirement. The standard tolerance is based on the International Tolerance (IT) grades table reference as ISO 286-1:2010 (2010). The recommended standard tolerance grade IT07 is followed as suggested by Feng et al. (2019).

3.1.1. Initial water saturation procedure before sample jacketing

This step of the test procedure is described in the following Figure 3. The major facilities include a vacuum pump, a syringe pump, a steel chamber that can hold high fluid pressure (up to several thousand psi), a water container, and a water cup. They are connected by a few pipes and valves (V1~ V6 in Figure 3).

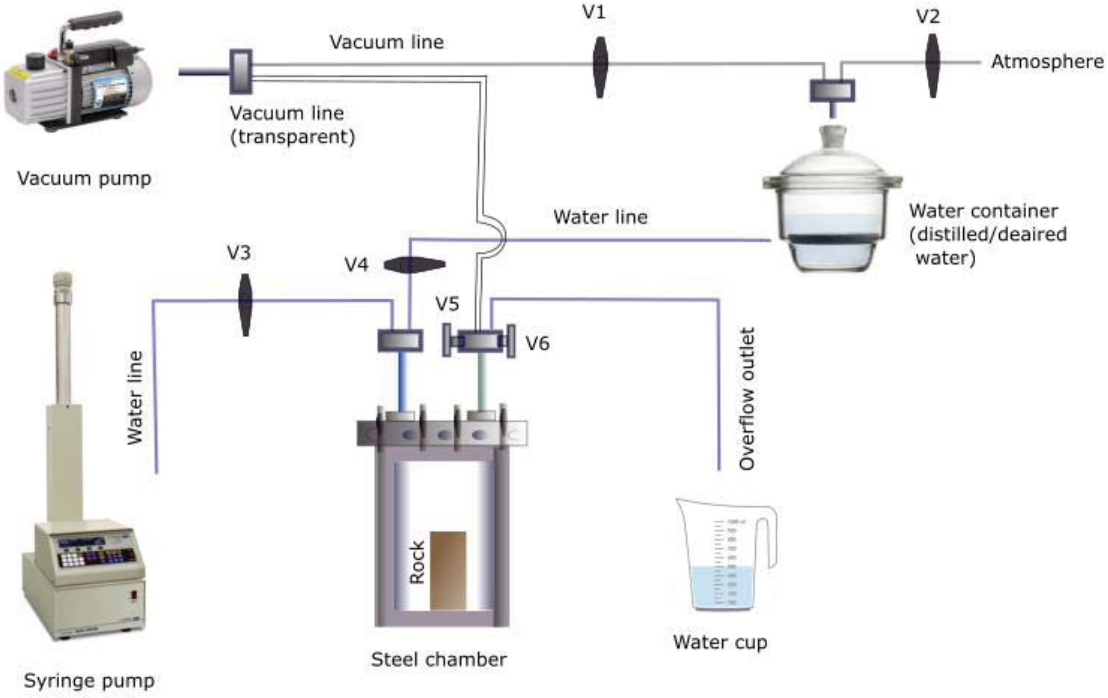

Fig.3 Schematic configuration for water saturation before sample jacketing.

1) Prepare distilled and de-aired water for use in the pore system including the rock sample, the syringe pump, the water container and the associated pipes. The distilled water is supplied by the OU Rock Mechanics laboratory system, and the water is further de-aired by a vacuum pump.
2) Put the dry rock sample in a steel chamber and close the lid and seal the lid with grease. The lid is specially designed with two holes allowing fluid communication with the external devices. Vacuum this chamber using a vacuum pump by opening Valve 5 while close all the other valves. Ensure water in the water container has also been de-aired. (Can also open Valve 1 to vacuum the water container at the same time if needed).
3) After two hours, close V1 (if it was opened), close V5, open V2 and then V4. The distilled/de-aired water in the water container will be sucked by the negative air pressure (-20 psi in this case) inside the steel chamber to submerge the sample.
4) After the chamber is almost full of water with the rock sample totally submerged under water, lock the lid with clamps and bolts. The lid can be opened before locking to double check the water level to ensure the sample is fully covered by water.
5) After the lid is locked, close V4, open V5, run the vacuum pump to create a negative pressure in the chamber (generally -20 psi) and then close V5 to remain a vacuumed condition for the sample.
6) After 1 day or so, open V4 and V5, run the vacuum pump to further suck the water from the water container to the steel chamber until water appears in the pipe above the valve V5. Note this section's pipe is transparent (use relatively stiff polyethylene pipe) to allow the observation of water overflow. Another option is to use steel pipe but add a water trap in this section between the pump and V5 to avoid water overflow into the vacuum pump.
7) Once water overflow detected, close V5 and V4, open V3 and V6, pump distilled/deaired water from the syringe pump into the chamber and allow at least 80~100 ml water overflow to the water cup. And then close V6.
8) Further pump water into the steel chamber by the syringe pump to increase the fluid pressure up to 1000 psi and maintain the pressure for one day at least (the time can be much longer if the schedule

is not tight). This pressure is believed to be high enough to be able to enhance the saturation for a low permeability rock.

9) During this time period, a fluid cycling process can be performed. Gradually reduce the fluid pressure to a very low level, open V6, and pump fresh de-aired water from the syringe pump to replace the old fluid in the steel chamber. Since both the inlet and outlet pipes are all connected on the lid, the fluid on the top region in the chamber will be replaced. If there is any trapped air in the chamber's fluid, the cycling is helpful to reduce the air concentration in the fluid. After a significant amount of fluid (at least 100 to 200 ml) overflowed to the water cup, the overflow line can be closed. Then, gradually increase the fluid pressure in the chamber to a high level (1000 psi) as before.

10) When the sample is ready for jacketing, gradually reduce the fluid pressure to the atmosphere condition and take the sample out of the chamber. Seal the sample with two platens on both end surfaces and very thin copper shim (0.076 mm) on the lateral surface with epoxy to cover the whole setup for sealing. Note the platens' empty space (holes in the platens) should also be filled with water before the sealing work. After the epoxy consolidates, put the sample into the MTS 810 cell, and move on to the next step.

3.1.2. De-airing procedure after sample jacketing/installation

This step is illustrated in Figure 4. This step aims to remove the air or at least reduce the air concentration as much as possible in the pore fluid system. The major facilities include MTS 810 core holder, a vacuum pump, four syringe pumps, a water container, an Agilent data acquisition system, a computer, two pressure transducers. They are connected and controlled by a few pipes and valves (V1~V5 in Figure 4). All the pore fluid related parts (drainage lines, pressure transducers, platens, syringe pumps) were flushed and filled with distilled/deaired water before sample installation in the MTS 810 core holder.

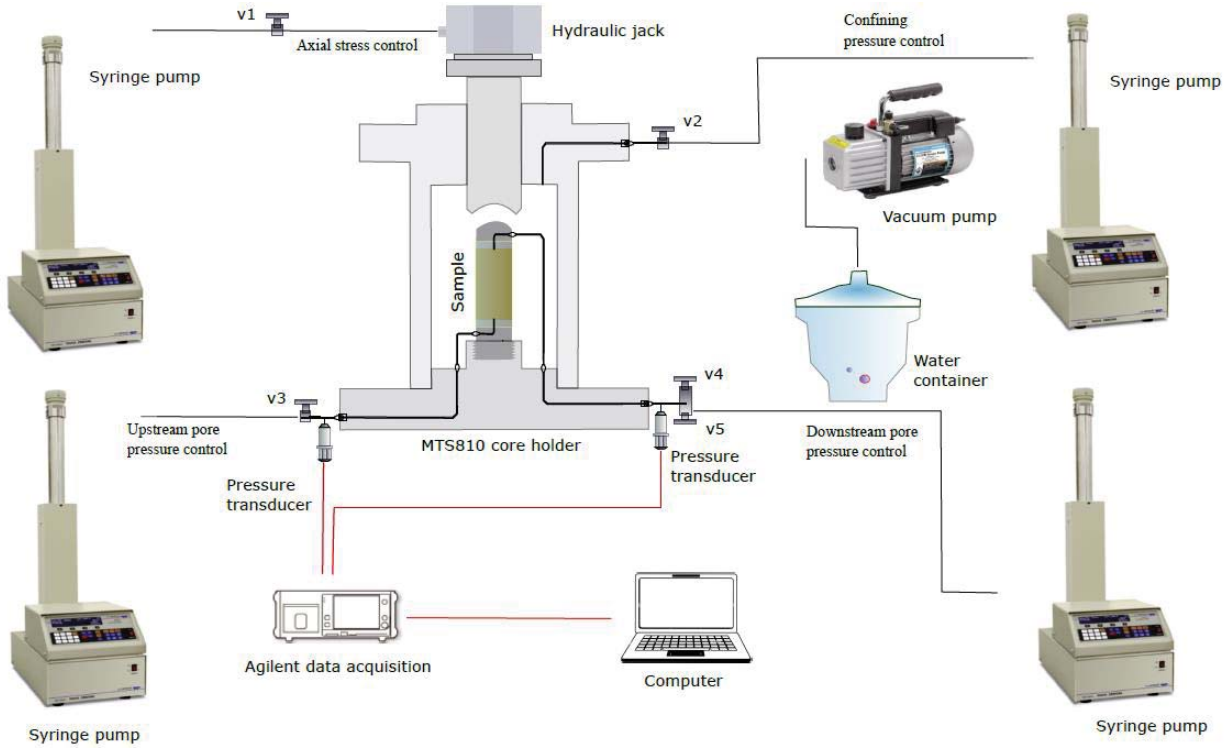

Fig.4 Schematic test configuration for Skempton's *B* measurement.

11) Connect the bottom platen with one syringe pump filled with distilled/deaired water (the upstream pump). Connect the top platen with a two-way valve (V4 and V5) which is further connected with a water container and a syringe pump, respectively; and connect this water container with a vacuum pump.
12) Close V1 and V5, open V2 to apply 500 psi confining pressure in the cell, and also apply 400 psi fluid pressure in the upstream pump with V3 opened. Open V4, create a negative pressure (-20 psi) in the water container by running the vacuum pump continuously.
13) Assuming the trapped air always tends to migrate upwards and is sucked by the vacuum pump, the fluid flow is expected to take the residual air out of the system. In fact, air foams can be observed in the chamber initially. The cover of the container is transparent to allow a direct observation of the inside of the container.
14) When no more air bubbles can be observed in the container, close V4, open V5. Increase confining pressure, upstream pump and downstream pump pressure to 1050 psi, 1000psi and 950psi, respectively. A low effective stress will allow a relatively high permeability in the sample. A high pore pressure is expected to further dissolve any trapped air in the rock. Allow a significant amount of water to flow through the sample. Depending on the rock permeability, fluid of 1~5 times of PV can pass through the sample within a reasonable time period (2~3 days or even longer). However, for an extremely low permeable rock such as Sierra White granite in this study, the core flooding process would be much longer. Thus using vacuum pump to suck the trapped air should be more frequent.
15) After a significant amount of pressurized flow has passed through the sample or at least 2~3 days' water flooding (in this case, one more week), reduce the pore pressure and confining pressure to 400 psi and 500 psi, respectively. Close V5, open V4, run the vacuum pump and check if there is any more air bubble in the water container. If some trace of air is still found, repeat the previous step. Otherwise, move on to the next step.

3.1.3. Skempton's *B* measurement under different backpressure but similar effective stress

Although efforts have been made to achieve a very high saturation of the sample and very low air concentration in the pore fluid, a full (100%) saturation of the sample without any trapped air may not be reached. There is a threshold pore pressure beyond which the Skempton's *B* will be insensitive to the fluid pressure, indicating a linear pore pressure measuring system. For a liquid (water), linear compressibility means the absence of free air (Mesri et al. 1976). The lower the threshold of the pore pressure to achieve such linearity, the higher the saturation degree of the sample with the pore fluid. Determination of the threshold of pore pressure for linear fluid compressibility and Skempton's *B* measurement is described below.

16) Ensure the valves V1 and V4 are closed, V2, V3 and V5 are opened. Set the upstream and downstream syringe pump pressures to the same value at 20 psi. Set the confining pressure at 100 psi, and the pore pressure can be taken as 20 psi under such a setting. Since the rock permeability is low, the pore pressure equilibrium inside the rock may take some time. Usually, a pore pressure equilibrium is indicated by a no flow condition between the rock sample and the pore pressure control pumps (both upstream and downstream pumps).
17) Close the valves V3 and V5. If the pore pressure as detected by the two pressure transducers (right outside of the cell with the red lines connecting with an Agilent data acquisition machine (Figure 4)) remain the same at 20 psi level (or less than 5% difference), a pressure equilibrium condition can be assumed to be reached under an undrained condition.
18) When the pore pressure equilibrium has been reached under an undrained condition (with valves V3 and V5 closed), increase the confining pressure from 100 psi to 150 psi, and record the change of pore pressure by the pressure transducers. The ratio between the pore pressure increment and the

confining pressure increment (50 psi in this case) is taken as the Skempton's *B* at this step corresponding to a back pressure at 20 psi.

19) Increase the pore pressure to 120 psi while also increase the confining pressure to 200 psi at the same time to ensure the confining pressure always higher than the pore pressure. After pore pressure equilibrium has been reached at this stage, further increase the confining pressure to 250 psi with the sample under an undrained condition. Record the corresponded pore pressure increase and get the Skempton's *B* at this step. Repeat the step (17) and (18) in a stepwise manner until successive values of the Skempton's B do not change.

The lowest pore pressure at a stage when the Skempton's *B* starts to level off can be taken as the pore pressure threshold when the pore fluid linearity is achieved. And this pore pressure can be set as the initial pore pressure (or backpressure) for the Skempton's *B* measurement under different effective stress levels (see the next Section 3.1.4). Figure 5 presents some typical curves to explain this part's work.

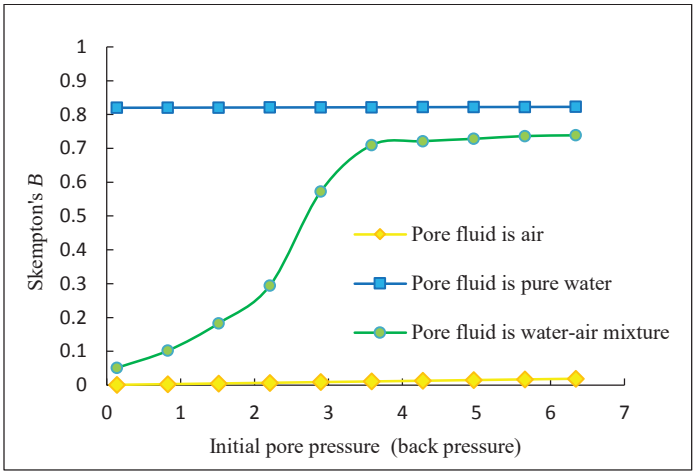

Figure 5. Typical Skempton's *B* behaviors with different types of pore fluids (when the pore fluid is air, Skempton's *B* is extremely low, close to zero; when the pore fluid is pure water, Skempton's *B* remains a relatively consistent high value; when the pore fluid is a mixture of water and air, it shows a curved line somewhere in between, and the shape and position of this line varies depending on the air concentration. When the air is totally dissolved into the water, the curve will asymptotically approach the pure water line).

However, if the test results show that there is significant air still trapped in the pore fluid system, one would need to repeat the steps in Section 3.1.2 and repeat the de-air procedure to further reduce the air concentration. Otherwise, move on to the next section to perform the measurement of Skempton's *B* with the focus on the rock matrix.

3.1.4. Skempton's *B* measurement under similar backpressure but different effective stress

This step aims to measure the Skempton's *B* at different effective stress condition and establish the correlation between the Skempton's *B* and effective stress. The initial pore pressure (back pressure) was set at a fixed value for each run and the confining pressure was increased stepwise; thus, the different Skempton's *B* is caused by the different effective stress and independent of the pore fluid compressibility because the fluid compressibility remains stable at a similar back pressure level. Generally, the threshold of the back pressure (initial pore pressure) for a well de-aired sample could be around 150~200 psi (Mesri et al. 1976). We usually use 500 psi (or above) as the back pressure for this work to ensure no free air exists in the pore fluid system.

20) Set both the upstream pump and downstream pump pressures at 600 psi (4.14 MPa) as the back pressure, set the confining pressure at 800 psi (5.52 MPa) and the pore pressure can be taken as 600

psi (4.14 MPa) when a pressure equilibrium condition between the sample and the pumps is reached. Note the pore pressure 600 psi (4.14 MPa) as used in this test is sufficiently high to ensure the consistent compressibility of the pore fluid during the measurement without any free air in the system. After pore pressure stabilization, shut off the valves (V3 and V5) to isolate the rock/pressure transducer system from the upstream/downstream pumps.

21) Increase the confining pressure quickly to a higher value and record the pressure transducer's reading, correspondingly. The ratio between pore pressure and confining pressure change will yield a Skempton's *B* value that's related with this effective stress (the difference between confining pressure and back pressure).
22) The test can be run at different starting points with similar back pressure (initial pore pressure) but different confining pressure (thus different effective stress). The difference of averaged confining pressure and pore pressure for a run can be taken as the effective stress in which the Skempton's *B* is related, and the stress dependency feature of the Skempton's *B* can be revealed after a series of tests with different starting points.

3.2. Biot's effective stress coefficient measurement

The schematic laboratory setup can be described in the following Figure 6. The major facilities include MTS 315 integrated cell and data acquisition system, Teledyne ISO syringe pumps, pore fluid storage tank, strain gauge measurement components. They are connected by a few pipes, valves, and signal lines.

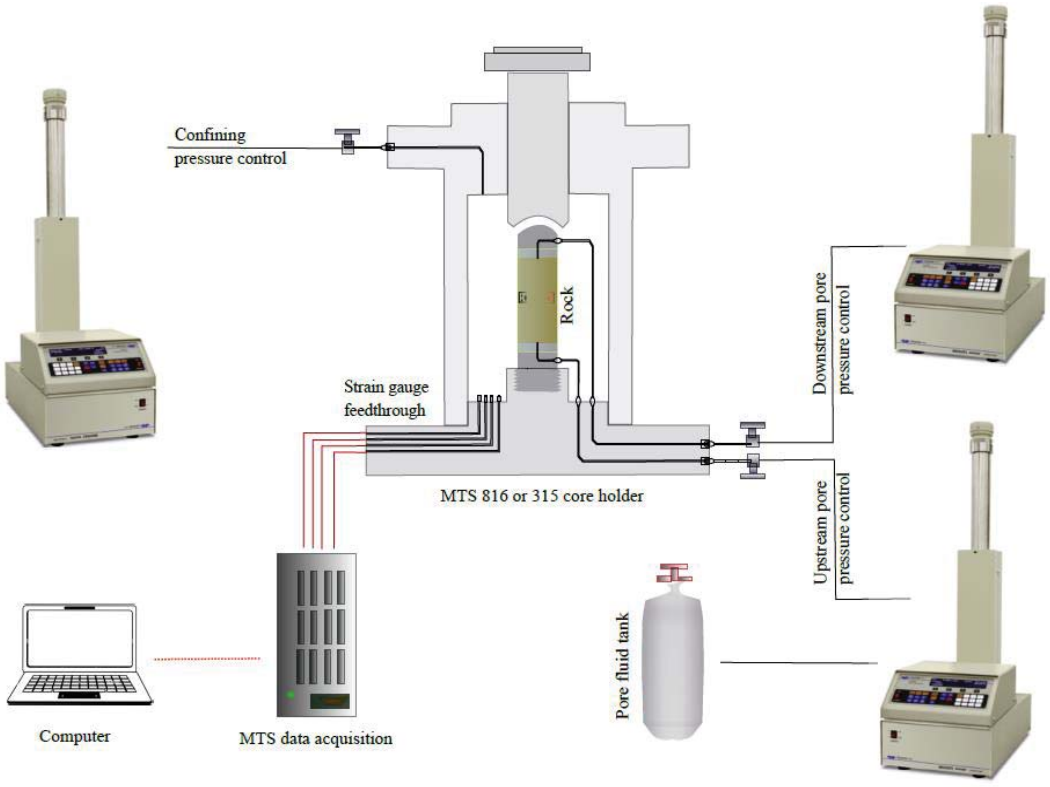

Fig.6 Test configuration for the Biot's effective stress coefficient measurement.

For this test, another dry Sample C was used. Since the sample's permeability is extremely low in the nano Darcy range, argon is used as the pore fluid. As an inert gas, argon has the advantage to ensure the pore pressure equilibrium in a relatively short time frame and also to avoid any physicochemical reactions between the rock matrix and the pore fluid, including the gas absorption effect and fines migrations during fluid flow, etc. The pore pressure was always kept at least 800 psi/5.52 MPa, which is above argon's

supercritical pressure (argon behaves more like a liquid above the critical point of 150K/-123 °C and 705 psi/4.86 MPa). Brace et al. (1968) showed that permeability tested by water on Westerly granite was similar to that by argon at high pore pressures when the argon is in its supercritical status.

1) Prepare a right cylindrical sample with a height-to-diameter ratio of 1.5~2.5 (in this case it is 1.8), which is in the favorable range for a conventional geo-mechanical testing (ISRM 2007; ASTM D4543-08 2008). The end face flatness (surface profile) is smooth to ±0.01 mm and free of any abrupt irregularities. The side of the specimen is also smooth and free of any abrupt irregularities.
2) Use two steel platens on both ends of the sample with circular porous sintered metal plate placed between the sample and the steel platen. Cover the lateral surface with ultrathin copper shim (0.003inch / 0.076 mm). Use epoxy to seal the whole setup. After the epoxy consolidates, put the sample into the core holder and apply high confining pressure (1000 psi/6.89MPa) to ensure the copper shim attached tightly on the sample surface. Ensure the sample is isolated from the confining fluid during this process.
3) After taking the sample out of the core holder, glue two sets of biaxial strain gauges on the lateral surface and ensure the axial direction of the gauge and the sample's vertical axis strictly in parallel. The volumetric strain is calculated by adding the averaged axial strain and two radial strains. In case some gauges yield nonlinear and/or extremely high or low values that is probably more a localized phenomenon, the experimenter may need to report both averaged results and the results by excluding those "abnormal" readings.
4) Put the sample in the core holder, connect the platens with the upstream/downstream pumps and the strain gauges with the feedthroughs. Check the signal quality and then close the cell.
5) For the purpose of the Biot's coefficient measurement, the grain bulk modulus, drained bulk modulus and the poroelastic expansion coefficient are needed. The grain bulk modulus is measured using a jacketed test with pore pressure always 100 psi lower than the confining pressure and recording the volumetric strain as measured by the strain gauges.
6) The drained bulk modulus K is a measure of the stiffness of the porous solid frame upon dry or constant pore pressure condition. While maintaining a constant pore pressure, the confining pressure is increased from a low level to high level and the strain is recorded during this process. The loading rate should be low enough to ensure a drained condition. The maximum effective stress should cover the in-situ effective stress level of the sample if the sample is from a deep depth.
7) Poroelastic expansion coefficient H is the ratio of pore pressure change over the volumetric strain under a constant confining pressure condition. H is the counterpart of K, but is measured under constant confining pressure by varying the pore pressure. Maintaining a constant confining pressure at high level, the pore pressure is set close to the confining pressure, and then decreases slowly to a low level. The volumetric strain is recorded during this process. The loading rate should be low enough to ensure the pore pressure decreases in a quasi-static manner. The poroelastic expansion coefficient H can be evaluated from the slope of the effective stress vs volumetric strain curve. The confining and pore fluid pressure are recorded by the Agilent data acquisition system at a frequency of one data point per second.

4. Laboratory test results

4.1. Skempton's *B* measurement

Following the laboratory test protocol described in Section 3.1.3, the test results are illustrated in the following Figures 7~11 and Table 3. In this test, the confining pressure and backpressure were initially set at 100 psi (0.69 MPa) and 20 psi (0.14 MPa), respectively. Then, under an undrained condition, a 50-psi (0.35 MPa) increment of confining pressure was applied to cause the pore pressure to increase to obtain a Skempton's B at this backpressure level. After that step, the sample returned to a drained condition, and the next backpressure level of 120 psi (0.83 MPa) under a confining pressure of 200 psi (1.38 MPa) was applied,

and the process was repeated in a stepwise manner until a backpressure of 920 psi (6.34 MPa) under a confining pressure of 1000 psi (6.89 MPa) was reached. Note the effective stresses remain at a constant low level of 80 psi (0.55 MPa) during the entire loading path.

At first, after the sample installation and some effort to reduce the air concentration in the pore fluid system, a series of the measurements of the Skempton's *B* by increasing the initial pore pressure (backpressure) and confining pressure stepwise has been conducted. One can see that the pore pressure responses in the upstream and downstream of the sample are different, with one side much more sensitive to the confining pressure increment than another side (Figure 7; Table 3 (1st run)); such difference indicates water at one side is better de-aired than another side, and further de-air work is needed. The Skempton's *B* behavior that is based on this stage of testing is summarized in Figure 8. Because of the very low permeability, the pore pressure responses on both sides of the sample are different, and independent with respect to each other under a quickly undrained condition.

The test results (Table 3, 1st run and Figures 7 and 8) clearly show that there is some air still trapped in the pore system after the sample installation and initial de-air process, especially in the downstream section. Thus, further de-air work had to be conducted, including a lengthy core flooding process and using the vacuum pump to suck the air out of the system in the downstream section.

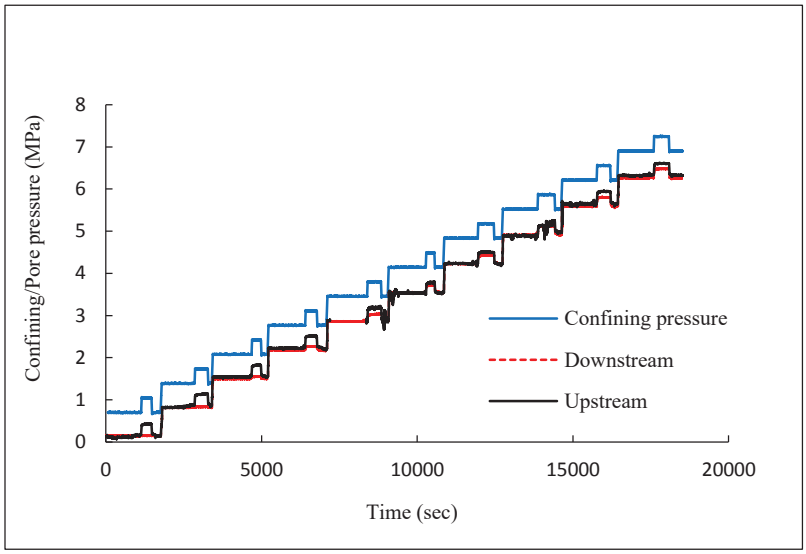

Fig.7 Skempton's *B* measurement after sample installation and initial de-aired work (in this loading path, the pore pressure responses to the confining pressure increase are different on the two sides of the sample, indicating one side (upstream) is better saturated with water than the other side (downstream); and further de-air work is needed on the downstream section to reduce the air concentration).

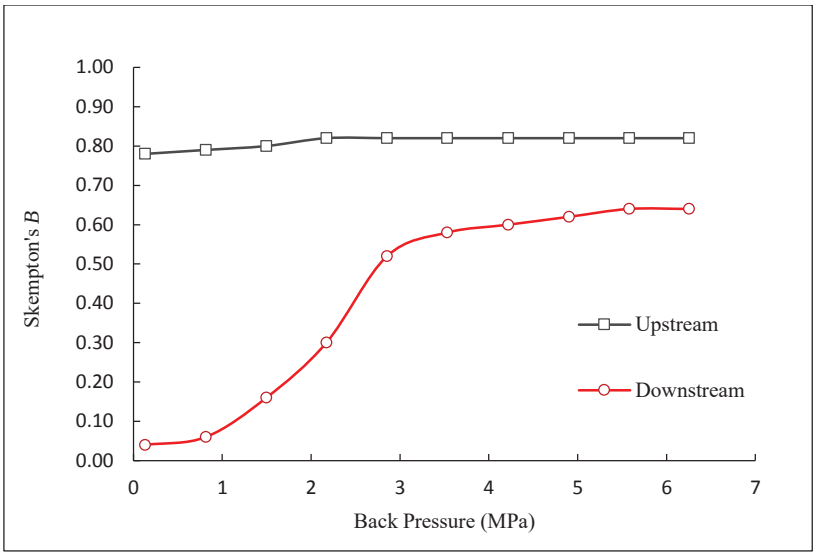

Fig.8 Skempton's *B* behavior based on Figure 7 (In the upstream section, the pore fluid is pure water thus yielding a consistent Skempton's *B* value; while in the downstream section, Skempton's *B* increases with the back pressures, indicating a condition of the pore water trapped with some air).

To verify if the pore water is air-free, another round of Skempton's *B* measurements similar to the first round of test was performed, and the test result is shown in the following Figure 9 and 10 and Table 3 (2nd run). Compare Figure 8 with Figure 10, the difference is obvious. In Figure 10, both sides of the sample respond to the confining pressure increase more promptly and similarly, and such responses are insensitive to the pressure levels, indicating the pore fluid system is depleted with air; a linear fluid compressibility has been achieved even at a very low back pressure level.

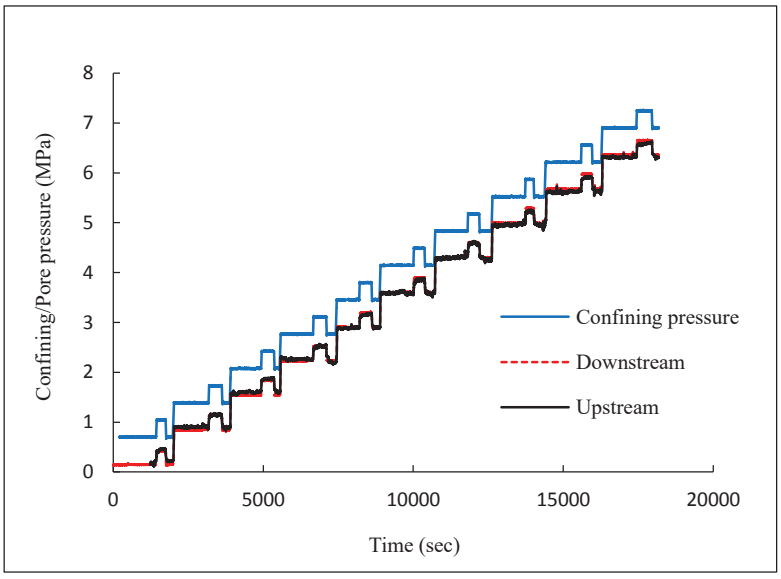

Fig. 9 Skempton's *B* test after further de-airing procedure (pore pressure response to the confining pressure increase is the same on both sides of the sample, and very sensitive to the confining pressure change even at very low-pressure level, indicating the pore fluid system is well de-aired. An air-free water saturation has been achieved).

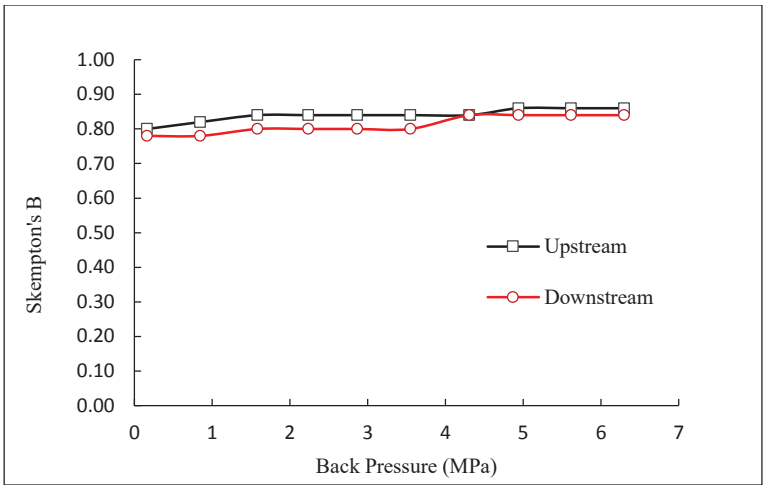

Fig.10 Skempton's *B* behavior based on Figure 9 (the change in downstream Skempton's B behavior is obvious to compare with Figure 7, indicating a condition of the pore fluid trapped with some air (Figure 8) and a condition with the pore fluid depleted from air (Figure 10)).

When there is air trapped in the pore water system, Skempton's *B* increases significantly from low pore pressure level to high pore pressure level because of the pore fluid compressibility changing greatly with the pore pressure when air exists in the pore system. However, once the air is depleted, the pore fluid compressibility tends to be constant, and insensitive to the pressure change. Skempton's *B* stabilized at 0.84 to 0.86 at high pressure levels for both sides. Note the effective stress for each round of test is all the same around 80 psi (0.55 MPa), which is very small. When there is air trapped in the pore fluid, the air concentration in the pore fluid system varies at different back pressure levels, thus the Skempton's *B* is not unique even the effective stress level was maintained the same (as shown in the first run in Table 3). However, once air is depleted from the system, the Skempton's *B* becomes much more consistent under such loading path with a consistent effective stress level (as shown in the second run in Table 3).

Table 3. Skempton's *B* measurement of Sierra White granite (Sample A) at different back pressure with similar effective stress levels.

Correlation between Skempton's *B* and back pressure - First run											
Test #	Effective stress		Back pressure	Confining Pressure Pc (psi)		Upstream fluid pressure Pp(psi)		Upstream Skempton's B	Downstream fluid pressure Pp(psi)		Downstream Skempton's B
	psi	MPa	MPa	start	end	start	end		start	end	
Test 1	79	0.54	0.15	100	150	24	63	0.780	19	21	0.040
Test 2	78	0.53	0.84	200	250	127	167	0.790	118	121	0.060
Test 3	79	0.54	1.52	300	350	225	265	0.800	217	225	0.160
Test 4	81	0.56	2.20	400	450	324	365	0.820	315	330	0.300
Test 5	81	0.56	2.89	500	550	425	466	0.820	414	440	0.520
Test 6	84	0.58	3.56	600	650	521	562	0.820	512	541	0.580
Test 7	87	0.60	4.23	700	750	615	656	0.820	612	642	0.600
Test 8	86	0.59	4.93	800	850	718	759	0.820	711	742	0.620
Test 9	88	0.61	5.60	900	950	815	856	0.820	809	841	0.640
Test 10	90	0.62	6.27	1000	1050	913	954	0.820	907	939	0.640

Correlation between Skempton's *B* and back pressure - Second run											
Test 1	77	0.53	0.16	100	150	22	62	0.800	24	63	0.780
Test 2	77	0.53	0.85	200	250	123	164	0.820	123	162	0.780
Test 3	74	0.51	1.56	300	350	223	265	0.840	230	270	0.800
Test 4	76	0.52	2.23	400	450	323	365	0.840	325	365	0.800
Test 5	81	0.56	2.89	500	550	422	464	0.840	416	456	0.800
Test 6	81	0.56	3.58	600	650	523	565	0.840	515	555	0.800
Test 7	76	0.52	4.31	700	750	624	666	0.840	625	667	0.840
Test 8	80	0.55	4.96	800	850	723	766	0.860	717	759	0.840
Test 9	81	0.56	5.65	900	950	823	866	0.860	815	857	0.840
Test 10	83	0.57	6.33	1000	1050	921	964	0.860	914	956	0.840

* Note Figure 7, 8 are the visualization of the 1st run, and Figure 9, 10 are for the 2nd run, respectively. In all these tests, the effective stress (= confining pressure − pore pressure) were very small, around 80 psi (0.55 MPa). The back pressure refers to the initial pore pressure at each stage.

Based on the test results (Figure 10), the fluid compressibility has shown a linear trend even at a very low pore pressure level after a lengthy de-aired work (less than 100 psi/0.69 MPa; Figure 10). However, to ensure good test results, a back pressure of 600 psi (4.14MPa) is taken as a threshold, above which full saturation of the sample with water is completely achieved (Note in Figure 10, there are still subtle increases of Skempton's *B* across 4 MPa for both the upstream and downstream measurements). Thus, in the ensuing tests for Skempton's *B*, the initial pore pressure for each test was set to 600 psi (4.14MPa). The test procedure for this part's measurement is detailed in Section 3.1.4. The test results are summarized in Figure 11 and Table 4.

Table 4. Skempton's *B* measurement of Sierra White granite (Sample A) at different effective stress under pure water saturation.

Test #	Confining pressure (psi)	Upstream measurement				Downstream measurement			
		Pore pressure (psi)	Effective stress		Skempton's *B*	Pore pressure (psi)	Effective stress		Skempton's *B*
			psi	MPa			psi	MPa	
1	800	590				590			
	1300	898	306	2.11	0.616	900	305	2.10	0.620
2	1000	592				593			
	1500	847	531	3.66	0.510	847	530	3.65	0.508
3	1500	601				597			
	2000	805	1047	7.22	0.408	808	1048	7.22	0.422
4	2000	604				592			
	2500	784	1556	10.73	0.360	764	1572	10.84	0.344
5	2500	600				596			
	3000	745	2078	14.33	0.290	747	2079	14.33	0.302
6	3000	601				591			
	3500	725	2587	17.84	0.248	704	2602	17.94	0.226
7	3500	626				623			
	4000	730	3072	21.18	0.208	717	3080	21.24	0.188
8	4000	603				606			
	4500	708	3595	24.79	0.210	691	3601	24.83	0.170
9	4500	609				592			

	5000	698	4097	28.25	0.178	672	4118	28.39	0.160
10	5000	607				606			
	5500	678	4608	31.77	0.142	670	4612	31.80	0.128
11	5500	590				589			
	6000	664	5123	35.32	0.148	650	5131	35.37	0.122
12	6000	603				598			
	6500	670	5614	38.71	0.134	655	5624	38.77	0.114
13	6500	586				591			
	7000	642	6136	42.31	0.112	638	6135	42.30	0.094
14	800	695				703			
	1300	1107	149	1.03	0.824	1105	146	1.01	0.804

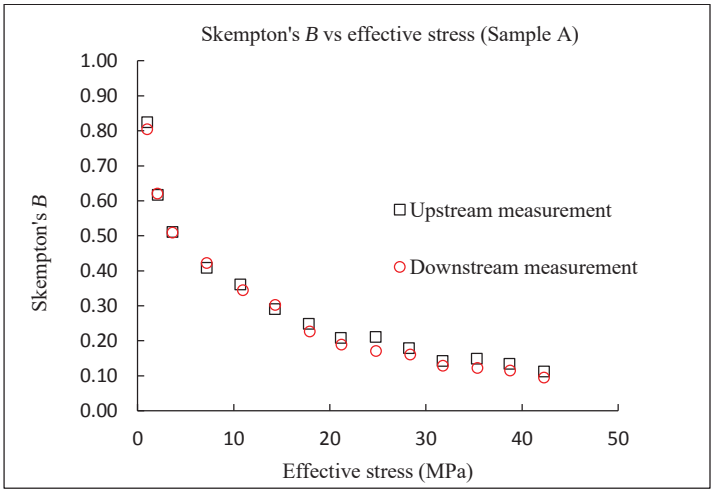

Fig.11 Skempton's *B* of Sierra White granite as a function of effective stress (the upstream and downstream values vary very slightly. The pore water has already been depleted of air as verified in the previous Skempton's *B* measurement (Figure 10)).

4.2. Biot's effective stress coefficient

This part's tests aim to measure the grain bulk modulus, $K_s^{'}$, drained bulk modulus, K, and the poroelastic expansion coefficient, H, from which the Biot's effective stress coefficient, α, can be derived.

4.2.1. Grain bulk modulus, $K_s^{'}$

The measurement was done starting at a confining pressure of 900 psi (6.21 MPa) and reaching to 5000 psi (34.47 MPa) and then decreasing to 1500 psi (10.34MPa). This was done in a stepwise manner using a pressure change of 100 psi (0.69 MPa) at each step. The pore pressure was maintained 100 psi lower than the confining pressure all the time. This stress path took a total of 6 days because of the low permeability of the sample. The waiting time for every increment must be long enough to allow pore pressure equilibrium in the sample. A way for detecting minimum waiting time is to observe the strain gauge readings, until these readings remain stable without any further change over the elapsed time.

For a rock sample with very low permeability, pore fluid equilibrium may not be able to be achieved during the loading path but is likely realized during the unloading path based on the past experience. A very long linear section appeared along the unloading path with a consistent slope (Figure 12), yielding a grain bulk modulus of 50.38 GPa, which is a reasonable result for the Sierra White granite by considering its mineral composition (Table 2).

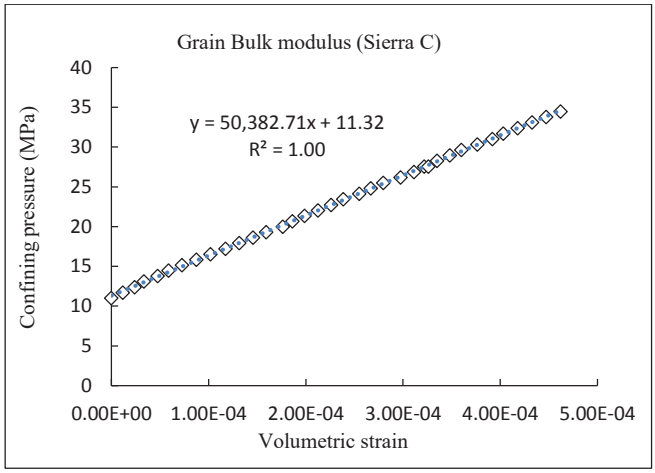

Fig.12 Grain bulk modulus measurement of Sierra White granite (50.38 GPa).

Sierra White granite was mainly made of two types of minerals, one is quartz (about 44%), and another is albite (about 46%) (Table 2). Quartz's bulk modulus is relatively low, about 37~40 GPa (Hart and Wang 1995; Wang 2000), while albite's bulk modulus is much higher, about 70 GPa but can also vary depending on a more detailed mineral phase (Ahrens 1995; Pabst et al. 2015). Thus, the grain bulk modulus as measured in this work, 50 GPa, is a reasonable estimation for this type of rock.

4.2.2. Drained bulk modulus, K

During the hydrostatic compression test, the loading curve usually shows a non-linear behavior, and consequently, bulk modulus can be separated into secant bulk modulus and tangent bulk modulus. Tangent parameter is used in view of the nonlinear response of rocks, since nonlinear tangent bulk modulus is highly stress dependent in comparison with secant bulk modulus. The tangent bulk modulus is approximated in a stepwise manner by calculating the slope of every small section along the loading path, and then the relationship between K and the corresponded effective stress can be established. Based on the Equation (4), the Biot's effective stress coefficient can be calculated, and its relationship with the effective stress can also be established. The test was performed under 800 psi (5.52 MPa) pore pressure (constant) with confining pressure increased from 1200 psi (8.27 MPa) to 6800 psi (46.89 MPa) within 25 hours at a loading rate of 3.8 psi/min. This loading rate is slow enough to maintain a drained condition. Figure 13 shows the drained bulk modulus test results; the curve is formed by 18,000 points with a data acquisition frequency of one point per five seconds.

4.2.3. Poroelastic expansion coefficient, H

The test was performed under 6400 psi (44.13 MPa) confining pressure with pore pressure decreasing from 6000 psi (41.37 MPa) to 1000 psi (6.89 MPa) within 27 hours at a constant loading rate of 3.3 psi/min. If the pore pressure path is transferred into effective stress path (effective stress = confining pressure - pore pressure), the following Figure 13 can be achieved. Figure 13 can make K and H to be tied by the similar effective stress.

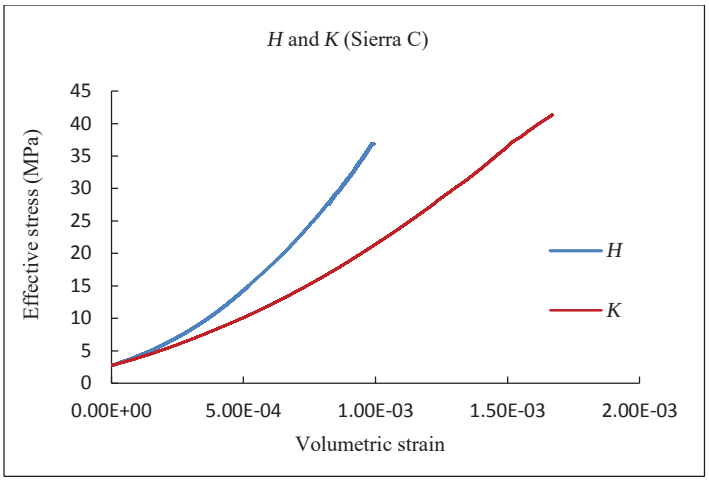

Fig.13 Drained bulk modulus *K* and poroelastic expansion coefficient *H* of Sierra White granite Sample C.

The two types of curves of K and H show similar features, i.e., all the curves show an increased slope over the increase of stress, and H curve generally has a higher slope than that of K curve. The Biot's coefficient can be evaluated by comparing K and H at the similar effective stress using Equation (5).

4.2.4. Biot's effective stress coefficient, α

The Biot's coefficient can be calculated based on the Equation (4) and (5), as that shown in Table 5 and Figure 14.

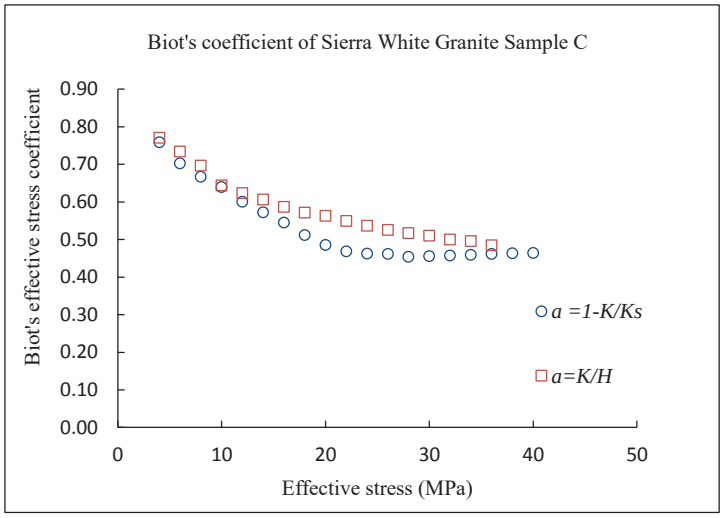

Fig.14 Biot's effective stress coefficient by two different approaches.

Table 5. Test result summary for the Biot's effective stress coefficient

Effective stress	K	K_s'	α	H	α
MPa	GPa	GPa	$1-K/K_s'$	GPa	K/H
4	12.12		0.76	15.72	0.77
6	14.98		0.70	20.39	0.73
8	16.78		0.67	24.07	0.70
10	18.14		0.64	28.16	0.64

12	20.12	50.38	0.60	32.27	0.62
14	21.55		0.57	35.52	0.61
16	22.92		0.55	39.08	0.59
18	24.57		0.51	42.97	0.57
20	25.93		0.49	46.03	0.56
22	26.75		0.47	48.69	0.55
24	27.08		0.46	50.43	0.54
26	27.12		0.44	51.57	0.53
28	27.51		0.46	53.17	0.52
30	27.41		0.46	53.74	0.51
32	27.33		0.46	54.66	0.50
34	27.24		0.46	54.96	0.50
36	27.11		0.46	55.88	0.49
38	27.01		0.46		
40	27.00		0.46		

Overall, the Biot's coefficient of the Sierra White granite sample decreases from 0.77 at low effective stress to 0.45~ 0.55 at high effective levels. The results from these two different approaches are not identical but close enough to establish confidence. Since rock is not a perfect homogeneous elastic material, there probably always exist some sort of variations among the different loading-unloading paths due to the inhomogeneity and inelasticity, which may lead to the minor difference for the Biot's coefficients as measured by different approaches.

5. Discussion and Conclusion

In this work a methodology has been developed and applied to measure the poroelastic properties including Skempton's *B* and the Biot's effective stress coefficient, α, of an ultra-low permeability rock namely, the Sierra White granite. Unlike the Biot's coefficient, which is only a solid phase property, Skempton's *B* is a property related to both the properties of solid rock material and the pore fluid. Thus, there are two types of Skempton's *B* behavior from the laboratory testing standpoint: one is related with the pore fluid compressibility (and can be tested under different backpressure with a constant low effective stress) and another related to the rock matrix (and can be tested under constant backpressure with different effective stresses). One may not be able to simply compare these two types of measurements as they reflect different mechanisms. For example, a low Skempton's *B* such as 0.3 found in the red curve (Figure 8) is caused by a low fluid compressibility, while a low Skempton's *B* of 0.3 in Figure 11 is caused by the low porosity and very stiff rock structure at higher effective stress. In fact, as has been suggested (Green and Wang, 1986), decreasing of the Skempton's *B* with increasing effective stress is related to the crack closure and/or high-compressibility materials within the rock framework.

At different back pressure but similar effective stress, the correlation between Skempton's *B* and pore pressure can reveal the impact of the pore fluid to Skempton's *B*. Increasing pore pressure will increase the pore fluid compressibility, thus Skempton's *B* will increase with the increase of pore pressure. However, if the pore fluid is depleted with air, the fluid compressibility will not be sensitive to the pore pressure change, and a leveled line will be present. Using this technique, one can determine if air is trapped in the pore fluid system and assess its severity. De-airing process should be implemented to reduce the air concentration in the pore fluid system to make the fluid as pure as possible, because Skempton's *B* is nonunique when the pore fluid compressibility varies. For a similar back pressure at different effective confining stress, the

correlation between Skempton's *B* and effective stress reveals the impact of rock matrix on Skempton's *B*. Increasing the effective stress reduces the porosity, thus decreasing the Skempton's *B*. Due to the existence of the dead volume (such as the thin hole in the platen and the pipe connected to the transducer outside of the rock sample, although efforts have been made to reduce such volume as small as possible such as filling with thin lead wire, this volume has not been totally removed), one may take the measurement as the lower limit of a "true" Skempton's *B* and data correction remains a task for the future (Bishop 1976).

The procedure described is a relatively complete testing protocol for the Skempton's *B* measurement, with the consideration of both pore fluid and rock matrix. The combination of these two types of Skempton's *B* measurements can give a more in-depth and complete understanding of the Skempton's *B* behavior for a rock sample. In fact, considering Equation (2), one can see that for the first type of measurement, the boundary condition is the constant effective stress which can guarantee the rock frame properties remain constant (K, $K_s^{'}$, $K_s^{''}$ and ϕ), thus the variation of *B* is caused by the change of K_f at different back pressures. While in the second type of measurement, the boundary condition is the constant back pressure that provides a constant K_f, then the change of K and ϕ at different effective stress can yield different values of *B*. Note $K_s^{'}$ and $K_s^{''}$ are generally insensitive to the stress change and can be taken as the constants from the laboratory testing standpoint.

For the Sierra White granite sample tested, the Biot's coefficient measurement, grain bulk modulus $K_s^{'}$ shows a linear behavior, while both drained bulk modulus K and poroelastic expansion coefficient H show nonlinear behaviors and are stress dependent. The measured grain bulk modulus of 50 GPa is appropriate for this sample by considering its mineralogical composition that are dominated by quartz and albite. Similarly, as that of Skempton's *B*, the Biot's effective stress coefficient also shows a stress dependent feature. The Biot's effective stress coefficient varies in a range of 0.77 down to 0.45~0.55 with the increase of the effective stress.

Declarations

Conflict of interest: The authors declare that they have no known competing financial interests or personal relationships that could have appeared to influence the work reported in this paper.

References

Ahrens TJ (1995) Mineral Physics and Crystallography: a handbook of physical constants. American Geophysical Union, Washington, DC.

ASTM (2004). Standard Test Method for Consolidated Undrained Triaxial Compression Test for Cohesive Soils. ASTM D4767.West Conshohocken, PA: ASTM.

ASTM D4543-08 (2008). Standard practices for preparing rock core as cylindrical test specimens and verifying conformance to dimensional and shape tolerances. American Society for Testing and Materials, West Conshohocken, PA.

Berge PA, Wang HF, Bonner BP (1993) Pore pressure buildup coefficient in synthetic and natural sandstones: International Journal of Rock Mechanics and Mining Sciences and Geomechanics Abstracts, Vol. 30, pp. 1135–1141. https://www.sciencedirect.com/science/article/abs/pii/014890629390083P

Berryman JG (2012) Poroelastic response of orthotropic fractured porous media: Transport in Porous Media, Vol. 93, pp. 293–307. https://link.springer.com/article/10.1007/s11242-011-9922-7

Berryman JG, Milton GW (1991) Exact results for generalized Gassmann's equations in composite porous media with two constituents: Geophysics, Vol. 56, pp. 1950–1960. https://library.seg.org/doi/10.1190/1.1443006

Biot MA (1941) General theory of three-dimensional consolidation. J Appl Phys 12(2):155–164.

https://aip.scitation.org/doi/10.1063/1.1712886
Biot MA, Willis DG (1957) The elastic coefficients of the theory of consolidation. J Appl Mech ASME 24:594–601. https://doi.org/10.1115/1.4011606
Bishop AW (1976). Influence of system compressibility on observed pore pressure response to an undrained change in stress in saturated rock. Géotechnique, 26(2), 371–375. https://doi.org/10.1680/geot.1976.26.2.371
Blocher G, Reinsch T, Hassanzadegan A, Milsch H, Zimmermann G (2014) Direct and indirect laboratory measurements of poroelastic properties of two consolidated sandstones. Int. J. Rock Mech. Min. Sci. 67:191-201. https://www.sciencedirect.com/science/article/abs/pii/S1365160913001482
Brace WF, Walsh JB, Frangos WT (1968) Permeability of granite under high pressure, J. Geophys. Res., 73, 2225–2236. https://doi.org/10.1029/JB073i006p02225
Brown RJS, Korringa J (1975) On the dependence of the elastic properties of a porous rock on the compressibility of the pore fluid: Geophysics, Vol. 40, pp. 608–616. https://doi.org/10.1190/1.1440551
Cheng AHD (1997) Material coefficients of anisotropic poroelasticity. Int J Rock Mech Min Sci 34(2):199–205. https://www.sciencedirect.com/science/article/abs/pii/S0148906296000551
Cheng AHD (2016) Poroelasticity, Theory and Applications of Tansport in Porous Media. Springer International Publishing Switzerland.
Coussy O (2004) Poromechanics. John Wiley & Sons, Ltd.
Feng X, Haimson B, Li X, Chang C, Ma X, Zhang X, Ingraham M, Suzuki K (2019) ISRM Suggested Method: Determining Deformation and Failure Characteristics of Rocks Subjected to True Triaxial Compression. Rock Mechanics and Rock Engineering (2019) 52:2011–2020. https://doi.org/10.1007/s00603-019-01782-z.
Ghassemi A, Tao Q, Diek A (2009) Influence of coupled chemo-poro-thermoelastic processes on pore pressure and stress distributions around a wellbore in swelling shale. J Pet Sci Eng 67(1–2):57–64. https://doi.org/10.1016/j.petrol.2009.02.015
Green HG, Wang HF (1986) Fluid pressure response to undrained compression in saturated sedimentary rock. Geophysics 1986;51(4):948–56. https://doi.org/10.1190/1.1442152
Hart DJ, Wang HF (1995) Laboratory measurements of a complete set of poroelastic moduli for Berea sandstone and Indiana limestone. J Geophys Res–Solid Earth 100(B9):17741–17751. https://doi.org/10.1029/95JB01242
Hu L, Ghassemi A (2020) Heat Production from Lab-scale Enhanced Geothermal Systems in Granite and Gabbro. Int. J. Rock Mech. Vol 126, ISSN 1365-1609. https://doi.org/10.1016/j.ijrmms.2019.104205
ISO 286-1-2010 (2010) Geometrical product specifications (GPS) — ISO code system for tolerances on linear sizes—part 1: basis of tolerances, deviations and fits.
ISRM (2007) The complete ISRM suggested methods for rock characterization, testing and monitoring: 1974–2006. In: Ulusay R, Hudson JA (eds) Suggested methods. prepared by ISRM commission on testing methods. Compilation Arranged by ISRM Turkish National Group, Ankara.
Jaeger JC, Cook NGW, Zimmerman RW (2007) Fundamentals of rock mechanics 4th edition. Malden, USA: Blackwell Publishing Ltd.
Makhnenko RY, Tarokh A, Podladchikov Y (2017) On the unjacketed moduli of sedimentary rock. In M. Vandamme, P. Dangla,J.-M. Pereira, & S. Ghabezloo (Eds.),Poromechanics VI—Proceedings of the 6th Biot Conference on Poromechanics, (pp. 897–904). AmericanSociety of Civil Engineers: Reston, VA. https://ascelibrary.org/doi/10.1061/9780784480779.111
Mesri G, Adachi K, Ullrich CR (1976) Pore-pressure response in rock to undrained change in all-round stress. Geotechnique, 26(2), 317-330. https://doi.org/10.1680/geot.1976.26.2.317
Pabst W, Gregorova E, Rambaldi E, Bignozzi MC (2015) Effective elastic constants of plagioclase feldspar aggregates in dependence of the Anorthite content – a concise review. Ceramics – Silikáty 59 (4) 326-330. https://www.ceramics-silikaty.cz/2015/pdf/2015_04_326.pdf
Rice JR, Cleary MP (1976) Some basic stress-diffusion solutions for fluid-saturated elastic porous media with compressible constituents: Reviews of Geophysics and Space Physics, Vol. 14, pp. 227–241. https://doi.org/10.1029/RG014i002p00227
Skempton AW (1954) The pore pressure coefficients A and B: Geotechnique, Vol. 4, pp. 143–147. https://doi.org/10.1680/geot.1954.4.4.143
Tarokh A, Detournay E, Labuz J (2018) Direct measurement of the unjacketed pore modulus of porous solids. Proceedings of the Royal Society A 474 (2219), 20180602. https://doi.org/10.1098/rspa.2018.0602
Wang HF (2000) Theory of Linear Poroelasticity with Applications to Geomechanics and Hydrogeology. Princeton University Press.
Ye Z, Ghassemi A (2018) Injection-Induced Shear Slip and Permeability Enhancement in Granite Fractures. Journal of Geophysical Research. https://doi.org/10.1029/2018JB016045

Zhou X, Vachaparampil A, Ghassemi A (2015) A Combined Method to Measure Biot's Coefficient for Rock. 49th US Rock Mechanics/Geomechanics Symposium held in San Francisco, CA, USA, 23-26, June 2015. https://onepetro.org/ARMAUSRMS/proceedings-abstract/ARMA15/All-ARMA15/ARMA-2015-584/65861

Zhou X, Ghassemi A, Riley S, Roberts J (2017). Biot's Effective Stress Coefficient of Mudstone Source Rocks. 51st US Rock Mechanics/Geomechanics Symposium held in San Francisco, California, USA,25-28 June 2017. 11p. https://onepetro.org/ARMAUSRMS/proceedings-abstract/ARMA17/All-ARMA17/ARMA-2017-0235/124216

Zhou X, Ghassemi A (2022) Experimental Determination of Poroelastic Properties of Utah FORGE Rocks. 56th US Rock Mechanics/Geomechanics Symposium held in Santa Fe, New Mexico, USA,26-28 June 2017. 12p. https://doi.org/10.56952/ARMA-2022-2137